

## Electrostatically Embedded Many-Body Approximation for Systems of Water, Ammonia, and Sulfuric Acid and the Dependence of Its Performance on Embedding Charges

Hannah R. Leverentz and Donald G. Truhlar\*

*Department of Chemistry and Supercomputing Institute, University of Minnesota,  
Minneapolis, Minnesota 55455-0431*

Received February 24, 2009

**Abstract:** This work tests the capability of the electrostatically embedded many-body (EE-MB) method to calculate accurate (relative to conventional calculations carried out at the same level of electronic structure theory and with the same basis set) binding energies of mixed clusters (as large as 9-mers) consisting of water, ammonia, sulfuric acid, and ammonium and bisulfate ions. This work also investigates the dependence of the accuracy of the EE-MB approximation on the type and origin of the charges used for electrostatically embedding these clusters. The conclusions reached are that for all of the clusters and sets of embedding charges studied in this work, the electrostatically embedded three-body (EE-3B) approximation is capable of consistently yielding relative errors of less than 1% and an average relative absolute error of only 0.3%, and that the performance of the EE-MB approximation does not depend strongly on the specific set of embedding charges used. The electrostatically embedded pairwise approximation has errors about an order of magnitude larger than EE-3B. This study also explores the question of why the accuracy of the EE-MB approximation shows such little dependence on the types of embedding charges employed.

### 1. Introduction

To compute properties of a chemical system often requires one to find a balance between computational cost and accuracy. A variety of relatively low-cost classical mechanical and semiempirical quantum mechanical methods allow one to calculate the properties of large (hundreds to thousands of atoms) systems quickly (sometimes within a fraction of a second), but, without problematic parametrization against experimental data, these methods are often incapable of providing more than qualitative accuracy for properties derived from a potential energy surface (PES). At the other extreme, calculations based on the first principles of quantum mechanics [such as coupled cluster<sup>1</sup> (CC) or configuration interaction<sup>2</sup> (CI) theory] have been developed that in principle could be carried to nearly arbitrary levels of quantitative accuracy<sup>3</sup> but that in practice may be used to calculate the energies only of systems containing a few atoms because of the methods' high computational cost. Thus, much

effort has been expended in order to find a broadly applicable method that can accurately calculate the energy of a large system at a cost that would be reasonable for use in either molecular dynamics (MD) or Monte Carlo (MC) simulations. Fragment-based approaches<sup>4–13</sup> are one class of methods that attempt to accomplish this goal. These methods involve breaking the large system into subsystems (which will be called fragments) that are small enough to be treated at some desired level of electronic structure theory. Often, an attempt is made to polarize each fragment by representing the “missing” fragments as point charges or continuous charge density distributions, and the large system's total energy is then calculated as some linear combination of the fragments' energies and sometimes of the energies of pairs and trimers of the fragments as well.

The electrostatically embedded many-body (EE-MB) method,<sup>13–17</sup> which will be described in greater detail in Section 2, is a relatively simple fragment-based method that is computationally inexpensive because it does not involve

the self-consistent determination of embedding point charges or charge distributions. In the formal EE-MB approximation, each fragment (or monomer), pair of fragments (dimer), and sometimes group of three or more fragments (trimer or higher oligomer), is embedded in a predetermined set of point charges (called embedding charges or background charges) that represents the fragments that are not explicitly included in the electronic structure calculation of a given monomer, dimer, or trimer. When tested on water clusters and on mixed clusters of water and ammonia, the EE-MB approximation showed itself to be a cost-effective way to accurately calculate the total energy of a system of noncovalently interacting molecules at virtually any desired level of electronic structure theory.<sup>13–17</sup> The present work continues to explore the EE-MB approximation by looking at two additional aspects of the EE-MB calculations, as described in the next two paragraphs.

First, the present study applies the EE-MB approximation to more complicated mixed systems than any on which it has yet been tested; the largest clusters considered in this article are formed from six water molecules, one ammonia molecule, and two sulfuric acid molecules. Clusters of this type were selected because these molecules are thought to be the fundamental components of clusters formed during the early stages of atmospheric nucleation processes.<sup>18</sup> In addition, these clusters test the EE-MB approximation's ability to predict accurate energies (compared to the "full" quantum mechanical calculation by the same electronic structure method) for systems involving both large and small fragments (the large fragment being sulfuric acid with five heavy atoms and the small fragments being water and ammonia with only one heavy atom each) as well as ions or charge transfer complexes because several of the configurations considered in this article correspond to clusters of ammonia, sulfuric acid, bisulfate ion, ammonium ion, and water rather than clusters of only ammonia, sulfuric acid, and water.

Second, the present study compares various ways to obtain the embedding charges and tests how sensitively the accuracy of the EE-MB approximation depends on the resulting sets of embedding charges. Typically the sets of background charges that represent the "missing" monomers are determined by performing some kind of population analysis or charge analysis on the electron density matrices of the isolated and optimized gas-phase monomers. Using these predetermined sets of background charges has several advantages relative to using charges that depend on the configuration under consideration: (1) it lowers the cost of the EE-MB calculation by precluding the need to perform additional self-consistent field calculations to determine the "best" background charges for each configuration, and (2) it maintains the straightforward availability of analytic gradients and Hessians (if they are already available for a given method of electronic structure theory) by removing the embedding charges' dependence on the specific geometry of the system. However, one might argue that using such an inflexible set of embedding charges may not adequately polarize each fragment and could potentially compromise the accuracy of the EE-MB approximation. Therefore, in the

present study we also test some inexpensive ways to obtain embedding charges that *do* depend on the specific geometry of each system being studied, and we compare the EE-MB results from those geometry-dependent (GD) charges with those from the geometry-independent (GI) charges that would be used in the formal EE-MB approximation. One should note that the formal EE-MB approximation would be more easily applied to dynamical simulations<sup>17</sup> that require fast calculations of PES gradients, but that either the formal EE-MB approximation or one that uses geometry-dependent background charges would be convenient for Monte Carlo simulations, where the calculation of PES gradients is not required.

The outline of the rest of this paper is as follows: Section 2 briefly reviews the theoretical underpinnings of the EE-MB approximation, Section 3 describes the computational methods used to perform the tests in this study and also gives the details of how the various sets of background charges were obtained, Section 4 presents the results and discusses their significance, and Section 5 summarizes our conclusions.

## 2. Theory

The EE-MB approximation, like several other fragment-based methods, is based on the many-body expansion of a system's total energy. Once a system has been fragmented into  $N$  monomers, the many-body expansion expresses the system's total energy as a sum of the energetic contributions of the one-body (i.e., individual monomer) interactions ( $V_1$ ), the two-body interactions ( $V_2$ ), the three-body interactions ( $V_3$ ), and so on up to the  $N$ -body term, as shown in eq 1.

$$E = V_1 + V_2 + V_3 + \dots + V_N \quad (1)$$

If one denotes the energy of one of the monomers as though it had the geometry it has in the cluster but were alone in a vacuum as  $E_i$  (where  $i$  runs over the arbitrary labels given to the monomers), the energy of dimer as  $E_{ij}$ , and the energy of a trimer as  $E_{ijk}$ , then the first three terms on the right-hand side of eq 1 are defined in eqs 2 through 4; the definitions of the remaining terms can be inferred from these equations.

$$V_1 = \sum_{i=1}^N E_i \quad (2)$$

$$V_2 = \sum_{i < j}^N (E_{ij} - E_i - E_j) \quad (3)$$

$$V_3 = \sum_{i < j < k}^N [E_{ijk} - (E_{ij} - E_i - E_j) - (E_{ik} - E_i - E_k) - (E_{jk} - E_j - E_k) - E_i - E_j - E_k] \quad (4)$$

One could approximate the total energy of the system by truncating eq 1 at some term  $V_M$  with  $M$  less than  $N$ ; this is the many-body (MB) approximation of the system's energy given by

$$E \approx V_1 + V_2 + V_3 + \dots + V_M \quad (5)$$

If one truncates eq 1 after  $M = 2$ , one has made the two-body (2B) or pairwise additive (PA) approximation. If one

truncates eq 1 after  $M = 3$ , one has made the three-body (3B) approximation.

The same equations as above underlie the EE-MB approximation, but the EE-MB approximation accounts for some of the higher-body interactions in the lower-order terms by calculating the monomer, dimer, trimer, etc. energies ( $E_i$ ,  $E_{ij}$ , and  $E_{ijk}$ ) as though each monomer, dimer, trimer, etc. were embedded in a field of point charges located at the coordinates of the missing nuclei. The surrounding point charges polarize or distort the electronic orbitals of each monomer (or group of monomers) so that they take on shapes and amplitudes that more closely resemble those that they might have in the overall system's wave function or electron density. Some of the specific methods by which such sets of embedding charges could be obtained are described in Section 3.

### 3. Methods

**3.1. Choices of Embedding Point Charges.** The paper that introduced the EE-MB approximation<sup>13</sup> pointed out that there are two major categories by which background charges may be determined for use in an EE-MB calculation: The first category, which yields what in this work we call the geometry-dependent or GD charges, calculates the density matrix corresponding to the wave function or the electron density function of the entire system at a computationally inexpensive level of electronic structure theory, such as the semiempirical method AM1,<sup>19</sup> and performs a charge analysis (such as a Mulliken,<sup>20</sup> Löwdin,<sup>21</sup> or redistributed Löwdin<sup>22</sup> analysis) on that density matrix to calculate partial charges located at the system's atomic centers. The second category, which yields what in this work we call the geometry-independent or GI charges, calculates the optimized density matrix of each type of monomer involved in the system and performs a charge analysis on each of those density matrices. The individual monomers can have their density matrices optimized in either the gas phase or a liquid solution phase. For example, if the system being studied were a cluster of water molecules, one could optimize a water molecule as though it were isolated in the gas phase or one could use an implicit solvation model to mimic an aqueous solution around the water molecule. The atom-centered partial charges calculated from each individually optimized density matrix are then used as the point charges representing that type of monomer in the EE-MB calculation, regardless of that monomer's position or shape in the overall system. The original (i.e., formal) EE-MB approximation calculates GI charges from monomers optimized in the gas phase, but we test the following three general types of point charges in the present work: GD charges, GI charges from monomers optimized in the gas phase, and GI charges from monomers optimized in a solution phase. (One could imagine another type of GD charge where charges are calculated for monomers but at the geometry they have in the particular configuration of the whole system that is under consideration, but we will not consider this method).

**3.2. Computational Methods.** All EE-MB calculations carried out in the present work were conducted using the

M06-2X<sup>23</sup> density functional, which was chosen because it performs better than other density functionals for noncovalent interactions between molecules composed of main-group elements.<sup>23</sup> Three different basis sets were used to test the overall accuracy of the EE-PA and the EE-3B approximation: MG3S,<sup>24</sup> cc-pV(T+d)Z+,<sup>25</sup> and aug-cc-pV(T+d)Z.<sup>26</sup>

In order to calculate the geometry-dependent (GD) sets of background charges, the AM1 wave function of each configuration studied was calculated, and the following methods of charge analysis were used on those wave functions: Mulliken population analysis,<sup>20</sup> Charge Model 1 (CM1A, where the A indicates that the version of CM1 used was specifically parametrized to be used with AM1 wave functions),<sup>27</sup> Charge Model 2 (CM2),<sup>28</sup> and Charge Model 3 (CM3).<sup>29,30</sup> One should note that Mulliken charges are Class II charges<sup>27</sup> and at best give electrostatic properties corresponding to an approximate level of theory with a finite set of basis functions, whereas CMx ( $x = 1A, 1P, 2, 3, 4$ , or 4M) charges are Class IV charges because they include empirical parameters that map Class II charges (such as Mulliken or Löwdin charges) to charges that more realistically reproduce experimental dipole moments. Following the recommendation of Udier-Blagović et al.,<sup>31</sup> a final set of GD charges has also been tested: these charges are simply CM1A charges scaled by 1.14, and they are labeled "CM1A\*1.14" or "scaled CM1A" charges. The scaling is designed to make the charges (although computed in the gas-phase) more appropriate for liquid simulations.

Geometry-independent (GI) charges were obtained from the density matrices of both gas-phase and liquid-phase monomers. The optimized density matrices of gas-phase monomers were used to calculate point charges according to eight different methods of charge analysis: ChEIPG,<sup>32</sup> Merz–Singh–Kollman (MK),<sup>33,34</sup> the MK method with the additional constraint to reproduce dipole moments as well as electrostatic potentials (ESP-Dipole; see the Gaussian 03 online manual<sup>35</sup> for details), Natural Bond Orbital (NBO),<sup>36</sup> CM1A, CM2, CM3, and CM4M.<sup>37,38</sup> NBO can be considered to be a Class II charge model, but rather than calculating charges from a density matrix expressed in terms of the original basis set functions, NBO charges are calculated from a density matrix expressed in terms of a set of functions that adopt the "natural" shapes that a chemist would expect to describe various types of chemical bonds. The ChEIPG, ESP-Dipole, and MK methods are quite similar to one another and yield what are classified as Class III charges; these charges are those that best reproduce the electrostatic potential due to a system's electron density distribution function at various points in space around the system (which is a gas-phase monomer for GI charge analysis). The ChEIPG, ESP-Dipole, MK, and NBO charges were determined from electron density functions computed by M06-2X/cc-pV(T+d)Z+//M06-2X/cc-pV(T+d)Z+ (we adopt the common notation  $W/X/Y/Z$ , where  $Y$  is the level of electronic structure theory or density functional and  $Z$  is the basis set with which the geometry of the system was optimized, and where  $W$  is the level of electronic structure theory or density functional and  $X$  is the basis set with which the electron density and/or energy to be used in subsequent calculations



was optimized). Because CM4M contains parameters that depend on the density functional and basis set chosen and is currently parametrized for a variety of double- $\zeta$  but not triple- $\zeta$  quality basis sets, the CM4M charges were calculated from the M06-2X/MIDI!//M06-2X/cc-pV(T+d)Z+ density matrix (the MIDI!<sup>39</sup> basis set is of double- $\zeta$  quality and was designed specifically for the efficient calculation of accurate geometries and partial charges). Charge Models 1, 2, and 3 were originally parametrized for semiempirical methods and to obtain the geometry-independent CM1A, CM2, and CM3 charges we used the AM1//AM1 wave functions of the isolated gas-phase monomers. The scaled CM1A charges (CM1A\*1.14) of the gas-phase monomers were also used as GI background charges for EE-MB calculations.

Three sets of background charges were based on liquid-phase monomers: these charges are denoted SM5.42/CM2, SM8/CM4M, and SMD/CM4M. To describe the density matrices used to obtain the charges, we adopt the following notation: *slvnt-SMx/W/X//slvnt-SMy/Y/Z*, where *W*, *X*, *Y*, and *Z* are as defined above and where *SMy* is the solvation model applied to perform a liquid-phase geometry optimization of the monomer, where *SMx* is the solvation model used to obtain a liquid-phase optimized wave (or density) function for subsequent charge analysis (for this study, *x* and *y* can be 5.42, 8, or D) and where *slvnt* indicates the solvent in which the monomer was theoretically immersed (for this study, *slvnt* = aq to signify that the calculation was performed in an aqueous solution). For SM5.42/CM2 charges, CM2 charges were calculated from the aq-SM5.42/AM1//AM1 monomer density matrices; that is, the monomer geometries were optimized by AM1 in the gas phase, and the wave functions were then optimized by AM1 in the aqueous phase using Solvation Model 5.42. “SM8” and “SMD” indicate Solvation Model 8<sup>40</sup> and Solvation Model D,<sup>41</sup> respectively. The SM8/CM4M charges are CM4M charges calculated from the aq-SM8/M06-L/6-31G(d)//M06-L/6-31G(d) monomer density matrices based on the M06-L density functional<sup>42</sup> with the 6-31G(d) basis,<sup>43,44</sup> and the SMD/CM4M charges are CM4M charges calculated from the aq-SMD/M06-L/6-31G(d)//M06-L/6-31G(d) monomer density matrices.

All geometries were optimized using the Minnesota Gaussian Functional Module, version 3.0 (MN-GFM-v3.0),<sup>45</sup> a locally modified version of the GAUSSIAN 03<sup>46</sup> electronic structure package, revision D.01. MN-GFM-v3.0 was also used to perform the charge analyses for the ChElPG, ESP-Dipole, MK, and NBO charges and to carry out single-point energy calculations on the clusters and molecules involved in this study. The Minnesota Gaussian Solvation Module, version 2008 (MN-GSM-v.2008),<sup>47</sup> a module for performing solvation calculations in GAUSSIAN 03, revision D.01, was used to compute the CM4M and SM8/CM4M charges. The SMD/M06-L/6-31G(d)//M06-L/6-31G(d) wave function was computed using the GESOL<sup>48</sup> program (an external module for GAUSSIAN 03), but the SMD/CM4M charges based on this wave function were computed using MN-GSM-v.2008. Calculations done on AM1 wave functions to find the geometry-dependent and geometry-independent CM1A, CM2, and CM3 charges as well as the geometry-independent

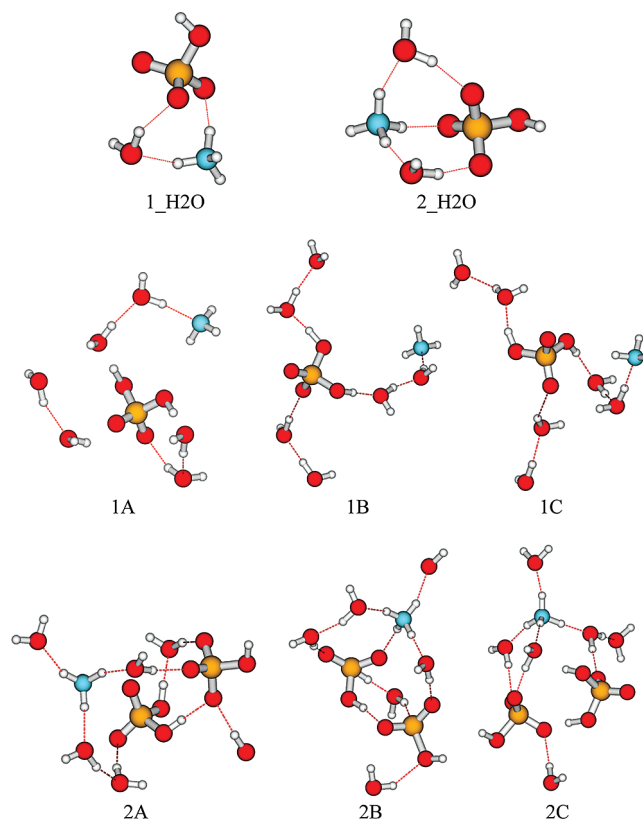


**Figure 1.** Eight clusters formed from water, ammonia, and sulfuric acid (note that many of the clusters contain ammonium and bisulfate ions rather than neutral ammonia and sulfuric acid molecules). The 1\_H2O and 2\_H2O structures were optimized at M06-2X/MG3S. The remaining structures were taken from molecular dynamics simulations. The composition of each cluster is as follows: (a) 1\_H2O = (HSO<sub>4</sub><sup>-</sup>)(NH<sub>4</sub><sup>+</sup>)(H<sub>2</sub>O), (b) 2\_H2O = (HSO<sub>4</sub><sup>-</sup>)(NH<sub>4</sub><sup>+</sup>)(H<sub>2</sub>O)<sub>2</sub>, (c) 1A = 1B = 1C = (H<sub>2</sub>SO<sub>4</sub>)(NH<sub>3</sub>)(H<sub>2</sub>O)<sub>6</sub>, and (d) 2A = 2B = 2C = (H<sub>2</sub>SO<sub>4</sub>)(HSO<sub>4</sub><sup>-</sup>)(NH<sub>4</sub><sup>+</sup>)(H<sub>2</sub>O)<sub>6</sub>.

SM5.42/CM2 charges were performed using AMSOL-version 7.1.<sup>49</sup> All EE-MB calculations were executed using MBPAC 2007-2,<sup>50</sup> a program that calls GAUSSIAN 03 or MN-GFM to perform electrostatically embedded many-body calculations.

## 4. Results and Discussion

The first goal of this study was simply to test how well the EE-PA and EE-3B approximations are able to reproduce the energies of systems containing water, ammonia, and sulfuric acid and/or their conjugate acids or bases calculated in the conventional manner for a given model chemistry (for this discussion, “model chemistry” or “method” implies a specific combination of electronic structure theory level or density functional with a specific basis set). To do this, the binding energies of eight clusters, each composed of between three and nine molecules, were calculated by M06-2X with three different basis sets: MG3S, cc-pV(T+d)Z+, and aug-cc-pV(T+d)Z.

The eight clusters considered in the first part of this work and their names are shown in Figure 1. The smallest cluster, called 1\_H2O, contains one bisulfate ion, one ammonium ion, and only one water molecule. Because the 1\_H2O cluster

**Table 1.** Binding Energies ( $E_{\text{bind}}$ , kcal/mol) of Eight Clusters with M06-2X Density Functional and Three Basis Sets and the Corresponding Errors<sup>a</sup> (kcal/mol) from the EE-PA and EE-3B Calculations using Five Different Sets of Geometry-Independent Background Charges

basis	system	$E_{\text{bind}}$ full	EE-PA errors					EE-3B errors				
			ChEIPG	ESP-dipole	MK	NBO	CM4M	ChEIPG	ESP-dipole	MK	NBO	CM4M
MG3S	1_H2O	-30.50	-0.57	-0.62	-0.59	-0.12	-0.98					
cc-pV(T+d)Z+	1_H2O	-29.69	-0.61	-0.65	-0.63	-0.17	-1.04					
aug-cc-pV(T+d)Z	1_H2O	-29.57	-0.34	-0.38	-0.36	-0.06	-0.66					
MG3S	2_H2O	-46.14	-1.36	-1.42	-1.36	-0.74	-1.87	0.06	0.06	0.06	0.02	0.06
cc-pV(T+d)Z+	2_H2O	-45.31	-1.43	-1.48	-1.43	-0.82	-1.96	0.03	0.04	0.03	-0.01	0.04
aug-cc-pV(T+d)Z	2_H2O	-45.08	-1.16	-1.20	-1.16	-0.65	-1.56	0.03	0.04	0.03	0.00	0.01
MG3S	1A	-52.23	1.11	1.17	1.06	0.04	2.19	0.17	0.17	0.17	0.11	0.22
cc-pV(T+d)Z+	1A	-51.80	1.14	1.18	1.08	0.01	2.23	0.15	0.15	0.14	0.10	0.19
aug-cc-pV(T+d)Z	1A	-50.87	1.23	1.31	1.17	-0.06	2.18	0.16	0.16	0.15	0.08	0.19
MG3S	1B	-31.39	0.48	0.50	0.44	-0.26	1.31	-0.06	-0.07	-0.06	-0.06	-0.05
cc-pV(T+d)Z+	1B	-31.80	0.50	0.51	0.45	-0.27	1.32	-0.05	-0.05	-0.05	-0.05	-0.04
aug-cc-pV(T+d)Z	1B	-30.89	0.53	0.58	0.48	-0.39	1.27	-0.04	-0.04	-0.04	-0.03	-0.03
MG3S	1C	-43.89	0.61	0.63	0.55	0.07	1.29	0.14	0.14	0.13	0.10	0.17
cc-pV(T+d)Z+	1C	-43.36	0.68	0.70	0.62	0.09	1.37	0.15	0.15	0.15	0.12	0.18
aug-cc-pV(T+d)Z	1C	-42.31	0.79	0.84	0.73	0.06	1.38	0.13	0.13	0.13	0.11	0.15
MG3S	2A	-66.84	-2.18	-2.23	-2.14	-1.58	-2.83	0.11	0.11	0.10	0.10	0.12
cc-pV(T+d)Z+	2A	-66.30	-2.21	-2.25	-2.16	-1.67	-2.82	0.14	0.13	0.13	0.12	0.15
aug-cc-pV(T+d)Z	2A	-65.24	-2.24	-2.28	-2.20	-1.76	-2.73	0.22	0.21	0.21	0.06	0.26
MG3S	2B	-68.53	-2.54	-2.61	-2.50	-1.79	-3.18	0.12	0.13	0.12	0.06	0.17
cc-pV(T+d)Z+	2B	-67.65	-2.63	-2.68	-2.58	-1.91	-3.23	0.14	0.14	0.13	0.07	0.20
aug-cc-pV(T+d)Z	2B	-66.71	-2.56	-2.60	-2.51	-1.83	-3.01	0.22	0.23	0.22	0.06	0.30
MG3S	2C	-62.70	-4.00	-4.15	-3.97	-2.55	-5.28	0.34	0.34	0.33	0.31	0.37
cc-pV(T+d)Z+	2C	-62.13	-4.03	-4.17	-3.99	-2.65	-5.27	0.29	0.29	0.27	0.26	0.30
aug-cc-pV(T+d)Z	2C	-61.29	-4.07	-4.22	-4.04	-2.58	-5.12	0.38	0.38	0.37	0.27	0.41

<sup>a</sup> The errors are calculated as  $E_{\text{bind}}(\text{EE-MB}) - E_{\text{bind}}(\text{full})$ .

contains only three molecules and because each molecule is defined as a monomer for the EE-MB calculations done in this study, only the EE-PA approximation is applied to this cluster (the EE-3B approximation necessarily yields the same result as the conventional calculation for the same method). The next smallest cluster contains one bisulfate ion, one ammonium ion, and two water molecules and is called the 2\_H2O cluster. Clusters 1\_H2O and 2\_H2O are based on structures shown in Figure 1 of ref 51; however, the precise coordinates used for the single-point energy calculations carried out in this study (which have been included in Supporting Information) were the result of M06-2X/MG3S geometry optimizations done on these two clusters. Six clusters, three of which comprise six water molecules, one ammonia molecule, and one sulfuric acid molecule and three of which comprise six water–water molecules, one ammonium ion, one bisulfate ion, and one sulfuric acid molecule, were also studied. These configurations are called 1A, 1B, 1C, 2A, 2B, and 2C. They were generated during an MD simulation;<sup>52</sup> a “1” in the name indicates that one sulfuric acid molecule was used in the starting configuration of the simulation, and a “2” indicates that two sulfuric acid molecules (one of which is in bisulfate form) were used in the starting configuration of the simulation.

The binding energy ( $E_{\text{bind}}$ ) of each of the clusters described in the preceding paragraph was first calculated in the conventional way with respect to the neutral gas-phase monomers with geometries optimized by the M06-2X/MG3S method. That is,

$$E_{\text{bind}} = E_{\text{cluster}} - \sum E_{\text{molecule}} \quad (6)$$

where  $E_{\text{cluster}}$  is the M06-2X/basis/M06-2X/MG3S absolute electronic energy of the cluster and  $E_{\text{molecule}}$  is the M06-2X/

basis/M06-2X/MG3S absolute energy of the neutral version of each molecule from which the cluster is formed [basis = MG3S, cc-pV(T+d)Z+, or aug-cc-pV(T+d)Z]. Table 1 lists the binding energy of each cluster when calculated in the conventional (or “full”) manner by each method and the difference (or error) between the EE-PA calculation with different sets of geometry-independent background charges calculated according to the formal EE-MB prescription; that is, the background charges were calculated from the optimized gas-phase monomers. These full binding energies were then used to test the truncated EE-MB expansions. Note that although the binding energies are defined with respect to the neutral versions of the monomers, in applying the EE versions of eqs 1–4 the clusters were fragmented into both neutral and ionic monomers and the background charges that were used to represent the missing monomers were calculated from the corresponding optimized gas-phase monomers, which are both neutral and ionic.

Table 1 shows that the EE-MB approximation, and in particular the EE-3B approximation, continues to yield accurate results when compared to the conventional calculations when it is used to calculate the binding energies of these more complicated clusters than others on which it has so far been tested. The maximum absolute error for the EE-PA calculations is 5.28 kcal/mol; this error occurs for structure 2C, which has a large binding energy, and so it corresponds to an error of only 8.4%. Furthermore, the average relative absolute error over all eight configurations, three basis sets, and five background charge sets for the EE-PA approximation is only 3.0%. The maximum absolute error for the EE-3B calculations (seven configurations) is a mere 0.41 kcal/mol, again for structure 2C, and it corresponds to a relative absolute error of only 0.7%. The average relative

absolute error over all seven configurations, three basis sets, and five background charge sets for the EE-3B approximation is 0.3%. These results imply that the EE-3B approximation is capable of handling complicated systems involving ions and/or charge transfer complexes and a wide range of monomer sizes and monomer complexity.

One particularly striking aspect of Table 1 is the comparative size of the EE-3B error in reproducing the full calculations and the deviations of the various full calculations from one another. Although all three basis sets are multiply polarized valence triple- $\zeta$  sets with diffuse functions, the results for a given cluster with a pair of basis sets differ from one another on average by 0.9 kcal/mol whereas a typical error due to the EE-3B approximation is  $\sim 0.1$  kcal/mol. Thus the error incurred by truncating the EE-MB expansion with geometry-independent background charges is much less than the uncertainty due to choice of basis set.

The second goal of this study was to compare two major categories of methods by which background charges for EE-MB calculations can be obtained: geometry-dependent and geometry-independent charges. From the geometry-independent charges, two subcategories of partial charge calculation methods are also compared: those that use the gas-phase monomer density matrices and those that use liquid-phase monomer density matrices. (See Section 3.1 for a more detailed explanation of these categories.) This portion of the study focuses on the binding energies of the three largest (and most complex) clusters (2A, 2B, and 2C) calculated by the M06-2X/cc-pV(T+d)Z+ method both conventionally and with the EE-MB approximation (MB = PA or 3B for this study) using background charge sets from each of the above categories and subcategories. [The cc-pV(T+d)Z+ basis set was selected because, of the three basis sets shown in Table 1, it is generally the most efficient at reducing basis set superposition error (BSSE); that is, on average the cc-pV(T+d)Z+ basis set yields about the same amount of BSSE as aug-cc-pV(T+d)Z but at lower cost.<sup>25</sup> The MG3S basis set tends to yield larger amounts of BSSE than the other two basis sets. Using a basis set that in general yields low BSSE diminishes the need to attempt to correct for BSSE by methods such as counterpoise correction,<sup>53</sup> which would significantly increase the overall cost of a calculation of the binding energy of a nine-molecule system.<sup>54</sup>]

Table 2 lists the errors from the EE-PA and EE-3B calculations relative to the conventionally calculated binding energy for each of the three clusters. The charge sets labeled with the prefix “GI\_” are geometry-independent charge sets; that is, these charges were calculated from the density matrices of individual monomers and therefore do not depend on a given cluster’s geometry (in still other words, these charge sets would remain the same for any cluster containing the same types of molecules and/or ions). Of the geometry-independent charge sets, those that were computed from aqueous-phase monomer density matrices contain the letters “SM” (for “solvation model”) in their labels immediately following the “GI\_” prefix; those that were computed from density matrices of gas-phase monomers do not. The “GD\_” prefix indicates that the given charge set is geometry dependent; that is, the charge set is calculated from a

**Table 2.** Binding Energies [ $E_{\text{bind}}(\text{full})$ , kcal/mol] from Conventional Calculations at M06-2X/cc-pV(T+d)Z+ and the Corresponding Errors<sup>a</sup> (kcal/mol) from the EE-MB Calculations When Different Sets of Background Charges Are Used

charge model	2A		2B		2C	
	EE-PA	EE-3B	EE-PA	EE-3B	EE-PA	EE-3B
$E_{\text{bind}}(\text{full})$	−66.30		−67.65		−62.13	
none <sup>b</sup>	−4.94	−0.85	−8.51	−0.14	−15.99	−1.11
GI_ChEIPG <sup>c</sup>	−2.21	0.14	−2.63	0.14	−4.03	0.29
GI_ESP-Dipole	−2.25	0.13	−2.68	0.14	−4.17	0.29
GI_MK	−2.16	0.13	−2.58	0.13	−3.99	0.27
GI_NBO	−1.67	0.12	−1.91	0.07	−2.65	0.26
GI_CM4M	−2.82	0.15	−3.23	0.20	−5.27	0.30
GI_CM1A	−2.29	0.14	−2.71	0.15	−4.21	0.31
GI_(CM1A*1.14)	−2.37	0.21	−2.76	0.23	−3.75	0.37
GI_CM2	−2.33	0.19	−2.83	0.16	−4.06	0.44
GI_CM3	−2.42	0.18	−2.93	0.17	−4.31	0.43
GI_SM5.42/CM2	−2.10	0.17	−2.50	0.12	−3.53	0.39
GI_SM8/CM4M	−2.40	0.14	−2.76	0.16	−4.36	0.26
GI_SMD/CM4M	−2.35	0.14	−2.70	0.15	−4.24	0.26
GD_AM1-Mulliken <sup>d</sup>	−2.96	0.18	−3.82	0.20	−6.42	0.52
GD_CM1A	−1.81	0.10	−2.04	0.08	−3.36	0.18
GD_CM1A*1.14	−1.98	0.15	−2.16	0.12	−2.85	0.21
GD_AM1-CM2	−1.79	0.11	−2.20	0.06	−3.67	0.29
GD_AM1-CM3	−1.80	0.11	−2.18	0.08	−3.50	0.26

<sup>a</sup> The errors are calculated as  $E_{\text{bind}}(\text{EE-MB}) - E_{\text{bind}}(\text{full})$ .

<sup>b</sup> “None” implies that no electrostatic embedding was used for these calculations; i.e., this row gives PA and 3B errors, not EE-PA and EE-3B errors. <sup>c</sup> The “GI\_” prefix indicates that these background charges are geometry independent. An “SM” following this prefix indicates that the charges were obtained from aqueous-phase monomers; all others were obtained from gas-phase monomers. <sup>d</sup> The “GD\_” prefix indicates that these background charges are geometry dependent.

semiempirical wave function for the entire cluster and therefore depends on the geometry of the cluster. Table 3 summarizes the results shown in Table 2 by listing the mean unsigned errors (MUE) and root mean squared errors (RMSE) of the EE-PA and EE-3B approximations over all three clusters. (Section 3.2 contains the specific description of the meaning of the name of each charge set and the method by which each charge set was calculated).

First, Tables 2 and 3 show that electrostatic embedding significantly enhances the accuracy of the PA and 3B approximations. Without electrostatic embedding, the pairwise additive MUE is 9.82 kcal/mol, whereas the maximum electrostatically embedded pairwise additive MUE is 4.40 kcal/mol and the average EE-PA MUE is 2.96 kcal/mol. Similarly, the three-body MUE without electrostatic embedding is 0.70 kcal/mol, whereas the maximum EE-3B MUE is 0.30 kcal/mol and the average EE-3B MUE is 0.20 kcal/mol.

A second point illustrated by Tables 2 and 3 is that GD charge sets yield EE-MB results that are only slightly better than those from GI sets. For the EE-PA approximation, the average GI MUE is 3.00 kcal/mol and the average GD MUE is 2.84 kcal/mol. For the EE-3B approximation, the average GI MUE is 0.21 kcal/mol and the average GD MUE is 0.18 kcal/mol. The small (nearly insignificant for the EE-3B approximation) improvement in accuracy afforded by the GD charge sets is not worth the loss of convenient analytic gradients when performing MD simulations, nor does it even seem to be worth the tiny relative increase in cost that would



**Table 3.** Mean Unsigned Errors (MUE) and Root Mean Squared Errors (RMSE) in kcal/mol over Three Configurations (2A, 2B, and 2C) of an (H<sub>2</sub>SO<sub>4</sub>)(HSO<sub>4</sub><sup>-</sup>)(NH<sub>4</sub><sup>+</sup>)(H<sub>2</sub>O)<sub>6</sub> System<sup>a</sup>

charge model	EE-PA		EE-3B	
	MUE	RMSE	MUE	RMSE
full	0.00	0.00	0.00	0.00
none <sup>b</sup>	9.82	10.84	0.70	0.81
GI_ChEIPG <sup>c</sup>	2.96	3.06	0.19	0.20
GI_ESP-Dipole	3.03	3.14	0.19	0.20
GI_MK	2.91	3.01	0.18	0.19
GI_NBO	2.08	2.12	0.15	0.17
GI_CM4M	3.77	3.92	0.22	0.23
GI_CM1A	3.07	3.18	0.20	0.22
GI_(CM1A*1.14)	2.96	3.02	0.27	0.28
GI_CM2	3.07	3.16	0.26	0.29
GI_CM3	3.22	3.32	0.26	0.29
GI_SM5.42/CM2	2.71	2.78	0.23	0.26
GI_SM8/CM4M	3.17	3.28	0.19	0.19
GI_SMD/CM4M	3.10	3.21	0.18	0.19
GD_AM1-Mulliken <sup>d</sup>	4.40	4.64	0.30	0.34
GD_CM1A	2.41	2.50	0.12	0.13
GD_CM1A*1.14	2.33	2.36	0.16	0.17
GD_AM1-CM2	2.56	2.68	0.15	0.18
GD_AM1-CM3	2.50	2.60	0.15	0.17

<sup>a</sup> The full (or conventional) and EE-MB calculations were performed by the M06-2X/cc-pV(T+d)Z+ method. <sup>b</sup> No background charges were used for these calculations; i.e., these are the PA and 3B approximations to the total energy without electrostatic embedding. <sup>c</sup> The "GI\_" prefix indicates that these background charges are geometry independent. An "SM" following this prefix indicates that the charges were obtained from aqueous-phase monomers; all others were obtained from gas-phase monomers. <sup>d</sup> The "GD\_" prefix indicates that these background charges are geometry dependent.

be incurred during MC simulations. Therefore, the original EE-MB approximation where the electrostatic embedding is based on GI charges continues to be the recommended approach for EE-MB calculations.

A third conclusion that may be drawn from Tables 2 and 3 is that using gas-phase monomer wave or density functions as a starting point for the determination of GI charges is just about as good as using charges derived from liquid-phase monomers. The average MUE of the charge sets obtained from gas-phase monomers is 3.01 kcal/mol for the EE-PA approximation and 0.21 kcal/mol for the EE-3B approximation. The average MUEs of the charge sets obtained from aqueous-phase monomers are 2.99 and 0.20 kcal/mol, respectively. This may come as a surprise because one might expect that the electron density around a monomer in a cluster would more closely resemble the electron density distribution of a solvated monomer than it would the electron density distribution of a gas-phase monomer. This is because a monomer in a cluster or a monomer in solution is polarized by the surrounding monomers and might experience more charge separation than would a monomer in the gas phase; i.e., charges derived from either a monomer in a cluster or a monomer in solution might take on more extreme magnitudes than charges derived from a monomer in the gas phase. However, this did not turn out to be the case. The charges derived from liquid-phase monomers were on the whole quite similar to those derived from gas-phase monomers, as shown in Tables 4–6. This explains why

**Table 4.** Geometry-Independent Background Charges (in e) Based on the Geometries of the Gas-Phase Monomers Optimized with the M06-2X/cc-pV(T+d)Z+ Method

molecule	atom type	ChEIPG <sup>a</sup>	ESP-dipole <sup>a</sup>	MK <sup>a</sup>	NBO <sup>a</sup>	CM4M <sup>b</sup>
H <sub>2</sub> O	O	-0.726	-0.709	-0.731	-0.930	-0.601
H <sub>2</sub> O	H	0.363	0.355	0.365	0.465	0.300
HSO <sub>4</sub> <sup>-</sup>	S	1.428	1.329	1.328	2.591	0.403
HSO <sub>4</sub> <sup>-</sup>	O	-0.700	-0.677	-0.676	-1.016	-0.423
HSO <sub>4</sub> <sup>-</sup>	H	0.372	0.378	0.375	0.472	0.289
H <sub>2</sub> SO <sub>4</sub>	S	1.164	1.042	1.049	2.602	0.499
H <sub>2</sub> SO <sub>4</sub>	O	-0.509	-0.482	-0.483	-0.910	-0.298
H <sub>2</sub> SO <sub>4</sub>	H	0.435	0.443	0.442	0.519	0.347
NH <sub>4</sub> <sup>+</sup>	N	-0.784	-0.834	-0.834	-0.859	-0.604
NH <sub>4</sub> <sup>+</sup>	H	0.446	0.458	0.458	0.465	0.401

<sup>a</sup> Charge analyses were done on the M06-2X/cc-pV(T+d)Z+ gas-phase monomer density matrices. <sup>b</sup> Charge analyses were done on the M06-2X/MIDI! gas-phase monomer density matrices.

**Table 5.** Geometry-Independent Background Charges (in e) Based on the Geometries of the Gas-Phase Monomers Optimized with the AM1 Method

molecule	atom type	CM1A <sup>a</sup>	CM1A*1.14 <sup>a</sup>	CM2 <sup>a</sup>	CM3 <sup>a</sup>	SM5.42/CM2 <sup>b</sup>
H <sub>2</sub> O	O	-0.706	-0.805	-0.711	-0.679	-0.783
H <sub>2</sub> O	H	0.353	0.402	0.356	0.340	0.392
HSO <sub>4</sub> <sup>-</sup>	S	1.433	1.634	2.878	2.491	2.934
HSO <sub>4</sub> <sup>-</sup>	O	-0.709	-0.808	-1.061	-0.963	-1.086
HSO <sub>4</sub> <sup>-</sup>	H	0.401	0.457	0.368	0.360	0.409
H <sub>2</sub> SO <sub>4</sub>	S	1.440	1.642	2.874	2.487	2.961
H <sub>2</sub> SO <sub>4</sub>	O	-0.601	-0.685	-0.937	-0.842	-0.974
H <sub>2</sub> SO <sub>4</sub>	H	0.481	0.548	0.438	0.439	0.468
NH <sub>4</sub> <sup>+</sup>	N	-0.514	-0.586	-0.793	-0.829	-0.792
NH <sub>4</sub> <sup>+</sup>	H	0.378	0.431	0.448	0.457	0.448

<sup>a</sup> Charge analyses were done on the AM1 gas-phase monomer density matrices. <sup>b</sup> Charge analyses were done on the SM5.42/AM1 aqueous-phase monomer density matrices.

**Table 6.** Geometry-Independent Background Charges<sup>a</sup> (in e) Based on the Geometries of the Gas-Phase Monomers Optimized by the M06-L/6-31G(d) Method

molecule	atom + label	SM8/CM4M	SMD/CM4M
H <sub>2</sub> O	O	-0.695	-0.708
H <sub>2</sub> O	H	0.347	0.354
HSO <sub>4</sub> <sup>-</sup>	S	0.751	0.775
HSO <sub>4</sub> <sup>-</sup>	O	-0.525	-0.534
HSO <sub>4</sub> <sup>-</sup>	H	0.350	0.361
H <sub>2</sub> SO <sub>4</sub>	S	0.875	0.867
H <sub>2</sub> SO <sub>4</sub>	O	-0.416	-0.418
H <sub>2</sub> SO <sub>4</sub>	H	0.393	0.401
NH <sub>4</sub> <sup>+</sup>	N	-0.584	-0.592
NH <sub>4</sub> <sup>+</sup>	H	0.396	0.398

<sup>a</sup> Charge analyses were done on the SMx/M06 L/6-31G(d) (x = 8, D) aqueous-phase monomer density matrices.

these charge sets produce similar results when used as the background charges in EE-MB calculations. Once again, the original EE-MB approximation (taking GI charges from monomers in the gas phase) remains the recommended approach because gas-phase monomer calculations are less costly (even if only by a little) than liquid-phase calculations and because potential ambiguity regarding which solvent to choose for monomers involved in mixed clusters is avoided when the gas-phase monomers are used to generate embedding charges.

**Table 7.** Dipoles<sup>a</sup> (in debye) of Individual Water Molecules within Different Configurations of an (H<sub>2</sub>SO<sub>4</sub>)(HSO<sub>4</sub><sup>−</sup>)(NH<sub>4</sub><sup>+</sup>)(H<sub>2</sub>O)<sub>6</sub> System from Various Point Charge Representations of Those Configurations

cluster label	monomer label	Mulliken	CM1A	CM1A*1.14	CM2	CM3
2A	2	1.39	2.26	2.58	2.24	2.21
2A	4	1.37	2.20	2.50	2.18	2.15
2A	5	1.58	2.47	2.81	2.43	2.42
2A	6	1.35	2.30	2.62	2.31	2.24
2A	7	1.23	2.13	2.42	2.12	2.06
2A	9	1.30	2.22	2.53	2.21	2.15
2B	2	1.48	2.40	2.74	2.37	2.34
2B	4	1.39	2.24	2.55	2.22	2.19
2B	5	1.39	2.20	2.51	2.17	2.16
2B	6	1.30	2.19	2.49	2.20	2.13
2B	7	1.25	2.24	2.55	2.24	2.16
2B	9	1.31	2.19	2.50	2.18	2.13
2C	2	1.54	2.46	2.81	2.39	2.40
2C	4	1.42	2.25	2.56	2.21	2.20
2C	5	1.34	2.19	2.50	2.18	2.14
2C	6	1.44	2.44	2.79	2.45	2.38
2C	7	1.21	2.12	2.42	2.12	2.05
2C	9	1.18	2.08	2.38	2.10	2.01
average (debye)		1.36	2.25	2.57	2.24	2.20
standard deviation (debye)		0.11	0.12	0.13	0.11	0.12
% standard deviation		8.0	5.2	5.2	4.7	5.4

<sup>a</sup> Dipoles are calculated with respect to each water molecule's center of nuclear charge.

To summarize the discussion of the results presented so far, one could simply state that the accuracy of the EE-MB approximation does not appear to be heavily dependent on the set of background charges chosen. Compared to the average binding energy of the three clusters, −65 kcal/mol, a 5% error would be 3.3 kcal/mol and a 1% error would be 0.65 kcal/mol. Thus, most of the EE-PA calculations yield MUEs of less than 5% and all of the EE-3B calculations yield MUEs of less than 1%, regardless of the charge model used in this study.

The reason for which the two subcategories of GI charges (gas-phase vs liquid-phase monomers) do not produce significantly different EE-MB results was addressed in an earlier paragraph, but one is still left to wonder why GI charges manage to do about as well as GD charges. In an attempt to understand this, one can investigate (1) how the dipoles of individual water molecules vary within a cluster and (2) how the dipole of an individual water molecule varies when the water molecule is embedded in different sets of point charges. Because water is a planar molecule and generally possesses close to *C*<sub>2v</sub> symmetry, its dipole is a good indicator of the extent to which the water molecule is polarized. (Note that the word “dipole” is used to mean “the magnitude of the dipole moment”.) If the dipoles of the water molecules in the entire cluster do not vary much (Test 1), then one can see how the “inflexible” charges from a gas-phase monomer could adequately mimic the effects of other water molecules in the cluster. Additionally, if the dipole of a single water molecule embedded in point charges does not vary much with different background charge sets (Test 2), then one can infer that the choice of background charges will not strongly impact an EE-MB calculation, because the purpose of the background charges is to polarize the monomers, dimers, trimers, etc. If the embedding charges do not have a strong effect on the polarization of a monomer, then it is unlikely that they would have a strong effect on the result of an EE-MB calculation.

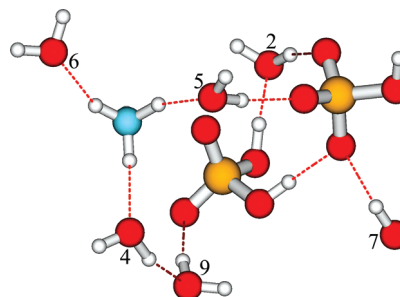


**Figure 2.** The 2A configuration with the water molecules labeled with the arbitrary fragment numbers that they were assigned for the EE-MB calculations. Note that two hydrogen atoms are obstructed from view in this figure: one is obstructed by the nitrogen atom of the ammonium ion, and the other is obstructed by the oxygen atom of water molecule 7.

As stated above, Test 1 investigates the variation in the dipoles of the water molecules within a given cluster. The dipole moment of each water molecule in clusters 2A, 2B, and 2C was calculated using the Mulliken, CM1A, scaled CM1A, CM2, and CM3 point charges that were obtained from the AM1 wave functions of those clusters; these dipoles are listed in Table 7. The point charges were used to calculate the dipoles because one cannot determine the expectation value of the dipole moment of an individual water molecule from the wave function of the entire cluster. The dipole moment of each water molecule was calculated with respect to that particular molecule's center of nuclear charge. To give an idea of the locations of the water molecules within a cluster, Figure 2 shows configuration 2A with each water molecule labeled by the arbitrary fragment number that it was assigned for the EE-MB calculations; these numbers correspond to the monomer labels listed in Table 7. The water molecules of configurations 2B and 2C were labeled in essentially the same way, although of course their locations within the cluster are slightly different in each case. Table 7 shows that for every type of point charge representation other



**Table 8.** Dipoles<sup>a</sup> (in debye) of Gas-Phase Monomers Calculated from Point Charges and Compared to Best Estimates

charge model	H <sub>2</sub> O	H <sub>2</sub> SO <sub>4</sub>	NH <sub>3</sub>	HSO <sub>4</sub> <sup>-</sup>	OH <sup>-</sup>	MUE <sup>b</sup>	RMSE <sup>b</sup>
ChEIPG	2.03	3.25	1.64	2.65	1.59	0.19	0.21
ESP-dipole	1.98	3.31	1.59	2.72	1.59	0.20	0.22
MK	2.04	3.27	1.67	2.68	1.59	0.21	0.22
NBO	2.60	3.70	1.89	3.24	2.20	0.68	0.70
CM4M	1.68	3.02	1.55	2.40	0.95	0.18	0.21
CM1A	2.02	2.25	1.76	1.83	1.38	0.40	0.49
CM1A*1.14	2.30	2.56	2.01	2.08	1.57	0.43	0.44
CM2	2.03	1.89	1.61	1.59	1.40	0.49	0.67
CM3	1.94	1.87	1.60	1.55	1.29	0.48	0.68
best estimate	1.85 <sup>c</sup>	2.96 <sup>d</sup>	1.47 <sup>e</sup>	2.60 <sup>f</sup>	1.33 <sup>f</sup>		

<sup>a</sup> The dipole of each compound was calculated with respect to the compound's center of nuclear charge. <sup>b</sup> The MUEs/RMSEs are averages of the differences between the point-charge derived and the best estimate dipoles over all five compounds. The MUEs/RMSEs are given in debye. <sup>c</sup> References 55–57. <sup>d</sup> Reference 58. <sup>e</sup> Reference 59. <sup>f</sup> Determined in the present study by a finite-field calculation at CCSD(T)/aug-cc-pV(T+d)Z//M06-2X/cc-pV(T+d)Z+.

than Mulliken charges, the relative standard deviation is only 5%. In the case of dipoles derived from Mulliken charges the relative standard deviation is 8%. These results indicate that the variation in the extent of polarization of water molecules in a semiempirical calculation of an entire cluster's wave function is not large.

Test 2 investigates the dependence of the extent of polarization of a single embedded water molecule on the choice of background charges. Monomer number 5 of configuration 2A was selected as the embedded water molecule for this test. The remaining water molecules were represented by the same sets of point charges described in Section 3.2, and the M06-2X/MIDI! density matrix of the water molecule in each charge set was calculated. From this density matrix, one can calculate the dipole of the water molecule in two different ways: (a) quantum mechanically as the expectation value of the dipole moment operator or (b) classically from a set of point charges that has been determined through charge analysis of the water molecule's density matrix. Dipoles computed by methods a and b are called density dipoles and point-charge dipoles, respectively.

Method b begs the question of which specific charge model should be used to assign point charges to the embedded water molecule. To decide which charge model to use for this specific task, the dipoles of several nonembedded gas-phase molecules and ions according to nine charge models listed in Table 8. The ChEIPG, ESP-Dipole, MK, and NBO charge analyses were carried out on the molecules' M06-2X/cc-pV(T+d)Z+ density matrices, the CM4M charges were determined from the M06-2X/MIDI! density matrices, and the CM1A, scaled CM1A, CM2, and CM3 charges were extracted from the AM1 wave functions. The geometries of these compounds had previously been optimized at the same level of theory at which the charge analyses were performed, except for the CM4M charges which had been optimized at M06-2X/cc-pV(T+d)Z+. The classical dipoles of these molecules calculated from these charge representations are shown in Table 8 and are compared to our best estimates of these dipoles. In the case of the neutral compounds, our best estimates are based on experimental values, but in the case

of ions these have been determined with respect to each given ion's center of nuclear charge by finite-field calculations done with the CCSD(T)/aug-cc-pV(T+d)Z//M06-2X/cc-pV(T+d)Z+ method. The MUEs and RMSEs over all five compounds with respect to the best-estimate dipoles are also given in Table 8. Based on the MUEs, the CM4M charges appear to reproduce the best estimate dipoles better than the other methods, so the CM4M charges of the embedded water monomer were used to calculate the classical dipoles of method b.

The dipoles arising from methods a and b are given in Table 9, along with the individual point charges used to calculate the dipoles for method b. One should first notice, by comparing the point charge dipole of the unembedded water molecule (in the row labeled "None") to the point-charge dipoles of the embedded water molecule, that the electrostatic embedding does increase the dipole of the water molecule by about 0.3 D. Once embedded, however, the specific background charge set chosen does not affect the point-charge dipole by more than 0.05 D (or the density dipole by more than 0.09 D). The relative standard deviations over all sets of embedding charges for the water molecule's CM4M charges, density dipoles (method a), and point-charge dipoles (method b) are all under 1.3%. Thus, the extent to which a water molecule is polarized is affected by whether or not the water molecule is embedded in point charges, but the extent of polarization does not depend heavily on the specific set of embedding charges used.

## 5. Conclusions

The primary goals of this paper were (i) to test the overall accuracy of the EE-MB approximation for clusters involving both large and small monomers as well as a mix of ions and neutral molecules and (ii) to observe the dependence of the EE-MB approximation's accuracy on the background charges used as the electrostatic embedding.

Regarding the first goal, this study shows that the EE-MB approximation is capable of providing accurate binding energies for relatively complicated systems. For five sets of embedding charges used with three different basis sets on a test set of mixed clusters ranging in size from two to nine molecules, the errors in the binding energies from the EE-PA approximation relative to the binding energies of the full calculations at the same level of theory do not exceed 10%, and in many cases are closer to 5%. The EE-3B approximation does even better, with relative errors that do not exceed 0.7%.

Regarding the second goal, this study shows (in accord with results from previous studies on less complicated systems<sup>13,16</sup>) that electrostatic embedding does significantly improve the performance of the PA and 3B approximations, but that the specific set of point charges used for the electrostatic embedding does not strongly influence the accuracy of the EE-PA or EE-3B approximations. Two general categories of background charge sets were tested: geometry-dependent (GD) and geometry-independent (GI) charge sets. On the whole, GD and GI charges yield EE-MB results of almost equal accuracy; over three configurations of a mixed nine-molecule system, the EE-3B MUE over

**Table 9.** CM4M Charges (in *e*) and Dipoles (in debye) of Monomer Number 5 from Configuration 2A Embedded in the Given Sets of Background Charges

background charges	H1 <sup>a</sup> ( <i>e</i> )	O ( <i>e</i> )	H2 <sup>b</sup> ( <i>e</i> )	density dipole <sup>c</sup> (D)	point-charge dipole <sup>d</sup> (D)
full <sup>e</sup>	0.321	−0.593	0.321	N/A <sup>e</sup>	1.87 <sup>e</sup>
none <sup>f</sup>	0.297	−0.596	0.298	1.95	1.76
GI_ChEIPG	0.371	−0.687	0.317	2.61	2.05
GI_ESP-dipole	0.371	−0.687	0.317	2.61	2.05
GI_MK	0.370	−0.687	0.317	2.61	2.05
GI_NBO	0.376	−0.690	0.314	2.63	2.06
GI_CM4M	0.366	−0.684	0.318	2.59	2.04
GI_CM1A	0.370	−0.686	0.315	2.60	2.05
GI_CM1A*1.14	0.380	−0.697	0.318	2.68	2.09
GI_CM2	0.377	−0.693	0.316	2.65	2.07
GI_CM3	0.375	−0.692	0.316	2.64	2.07
GI_SM5.42/CM2	0.377	−0.692	0.315	2.64	2.07
GI_SM8/CM4M	0.367	−0.684	0.317	2.59	2.04
GI_SMD/CM4M	0.368	−0.684	0.317	2.59	2.04
GD_Mulliken	0.378	−0.690	0.312	2.63	2.07
GD_CM1A	0.371	−0.684	0.313	2.59	2.05
GD_CM1A*1.14	0.380	−0.696	0.316	2.68	2.08
GD_CM2	0.377	−0.689	0.311	2.62	2.06
GD_CM3	0.377	−0.690	0.314	2.63	2.07
Average <sup>g</sup>	0.374	−0.689	0.315	2.62	2.06
standard deviation <sup>g</sup>	0.005	0.004	0.002	0.03	0.01
% standard deviation <sup>g</sup>	1.2	0.6	0.7	1.1	0.7

<sup>a</sup> The hydrogen atom (of monomer 5, see labels in Figure 2) that forms an H-bond with an oxygen atom of the nearby HSO<sub>4</sub><sup>−</sup> ion. <sup>b</sup> The hydrogen atom (of monomer 5) that is not involved in an H-bond. <sup>c</sup> Dipole calculated from the M06 2X/MIDI! wave function of the embedded water molecule. One D ≡ 1 debye. <sup>d</sup> Dipole calculated from the point charges given in the columns labeled H1, O, and H2. One D ≡ 1 debye. <sup>e</sup> The CM4M charges assigned to the water molecule when the M06-2X/MIDI! calculation is performed on the entire 2A configuration. Because in this case the sum of the point charges on this fragment is not zero, the point charge dipole moment was calculated with respect to this fragment's center of nuclear charge. <sup>f</sup> "None" indicates that water monomer 5 was left in the geometry that it has in configuration 2A but that it was not embedded in point charges. <sup>g</sup> The values found in the rows labeled "full" and "none" were not included in the calculations of the averages, standard deviations, or % standard deviations.

the GI charge sets is 0.21 kcal/mol and over GD charge sets is 0.18 kcal/mol. Although the GD charge sets perform slightly better, they are also slightly more complicated to implement for energies and much more complicated to implement for gradients. Of the GI charge sets, those that were obtained from gas-phase monomer density matrices do not perform significantly differently than those that were obtained from liquid-phase monomer density matrices: over the EE-3B binding energies of three configurations of the nine-molecule system, the gas-phase monomer-derived charge sets yielded an MUE of 0.21 kcal/mol, and the liquid-phase monomer-derived charge sets yielded an MUE of 0.20 kcal/mol.

A third objective that arose during the course of this study was to investigate why the GD charge sets do not perform as much better than the GI charge sets as one might have expected. The conclusions reached from that portion of the study are these: (1) The polarization of the water molecules within a given nine-molecule cluster does not vary much from molecule to molecule, implying that the "rigid" point charges from a gas-phase monomer are adequate to represent that type of monomer regardless of where it is located within a cluster. (2) The polarization of a water molecule is affected by the presence of embedding charges, but the specific set of embedding charges used does not strongly affect the extent of the water molecule's polarization. The purpose of the background charges in an EE-MB calculation is to include higher-order effects in lower orders of the many-body expansion through the polarization of individual monomers and groups of monomers. Because the extent to which a water molecule is polarized is not greatly influenced by the

**Table 10.** Mean Unsigned Errors in kcal/mol over Three Configurations of an (H<sub>2</sub>SO<sub>4</sub>)(HSO<sub>4</sub><sup>−</sup>)(NH<sub>4</sub><sup>+</sup>)(H<sub>2</sub>O)<sub>6</sub> System<sup>a</sup>

	MB	EE-MB
one-body approximation	205.9	231.1
two-body approximation	9.8	3.0
three-body approximation	0.7	0.2

<sup>a</sup> M06-2X/cc-pV(T+d)Z+; see Table 3. The EE-MB results in the present table are averaged over the 12 geometry-independent charge models of Table 3.

choice of embedding charges, one can understand why the overall accuracy of the EE-MB approximation is not greatly influenced by the choice of embedding charges.

As far as implications for future work, the most significant result of the present study is shown in Table 10, which shows results for the most complex systems in this article, namely the three 9-mers, each consisting of six water molecules, one ammonium ion, one bisulfate ion, and one sulfuric acid molecule. We see that the errors in the EE-MB approximation are very small, even for this complex cluster, and even with geometry-independent partial charges.

A concise summary of the major conclusions reached by this study is as follows: the EE-3B approximation as it was originally formulated (i.e., using geometry-independent background charges derived from equilibrium gas-phase monomer wave or density functions) can be trusted to provide accurate results for relatively complicated systems of widely varying sizes involving both ions and noncovalently interacting monomers.

**Acknowledgment.** The authors are grateful to the Minnesota Supercomputing Institute ([www.msi.umn.edu](http://www.msi.umn.edu)) for computer time. This work was supported in part by the National Science Foundation grant no. CHE07-04974.

**Supporting Information Available:** Tables listing the Cartesian coordinates of the eight structures shown in Figure 1 are available free of charge via the Internet at <http://pubs.acs.org>.

## References

- (1) Cizek, J. *J. Chem. Phys.* **1966**, *45*, 4256.
- (2) Shavitt, I. In *Methods of Electronic Structure Theory*; Schaefer, H. F. I., Ed.; Plenum: New York, 1977; pp 189–275.
- (3) Bytautas, L.; Matsunaga, N.; Nagata, T.; Gordon, M. S.; Reudenberg, K. *J. Chem. Phys.* **2007**, *127*, 204301.
- (4) Kitaura, K.; Ikeo, E.; Asada, T.; Nakano, T.; Uebayasi, M. *Chem. Phys. Lett.* **1999**, *313*, 701.
- (5) Deev, V.; Collins, M. A. *J. Chem. Phys.* **2005**, *122*, 154102.
- (6) Hirata, S.; Valiev, M.; Dupuis, M. X.; S., S.; Sugiki, S.; Sekino, H. *Mol. Phys.* **2005**, *103*, 2255.
- (7) Chen, X. H.; Zhang, J. Z. H. *J. Chem. Phys.* **2006**, *125*, 44903.
- (8) Jiang, N.; Ma, J.; Jiang, Y. *J. Chem. Phys.* **2006**, *124*, 114112.
- (9) Li, W.; Li, S.; Jiang, Y. *J. Phys. Chem. A* **2007**, *111*, 2193.
- (10) Fedorov, D. G.; Kitaura, K. *J. Phys. Chem. A* **2007**, *111*, 6904.
- (11) Xie, W.; Song, L.; Truhlar, D. G.; Gao, J. *J. Chem. Phys.* **2008**, *128*, 234108.
- (12) Hirata, S. *J. Chem. Phys.* **2008**, *129*, 204104.
- (13) Dahlke, E. E.; Truhlar, D. G. *J. Chem. Theory Comput.* **2007**, *3*, 46.
- (14) Dahlke, E. E.; Truhlar, D. G. *J. Chem. Theory Comput.* **2007**, *3*, 1342.
- (15) Dahlke, E. E.; Leverentz, H. R.; Truhlar, D. G. *J. Chem. Theory Comput.* **2008**, *4*, 33.
- (16) Sorkin, A.; Dahlke, E. E.; Truhlar, D. G. *J. Chem. Theory Comput.* **2008**, *4*, 683.
- (17) Dahlke, E. E.; Truhlar, D. G. *J. Chem. Theory Comput.* **2008**, *4*, 1.
- (18) Kulmala, M. *Science* **2003**, *302*, 1000.
- (19) Dewar, M. J. S.; Zebisch, E. G.; Healy, E. F.; Stewart, J. J. P. *J. Am. Chem. Soc.* **1985**, *107*, 3902.
- (20) Mulliken, R. S. *J. Chem. Phys.* **1955**, *23*, 1833.
- (21) Baker, J. *Theor. Chim. Acta* **1985**, *68*, 221.
- (22) Thompson, J. D.; Xidos, J. D.; Sonbuchner, T. M.; Cramer, C. J.; Truhlar, D. G. *PhysChemComm* **2002**, *5*, 117.
- (23) Zhao, Y.; Truhlar, D. G. *Theor. Chem. Acc.* **2008**, *120*, 215.
- (24) Lynch, B. J.; Zhao, Y.; Truhlar, D. G. *J. Phys. Chem. A* **2003**, *107*, 1384.
- (25) Papajak, E.; Leverentz, H. R.; Zheng, J.; Truhlar, D. G. *J. Chem. Theory Comput.*, in press.
- (26) Dunning, T. H., Jr.; Peterson, K. A.; Wilson, A. K. *J. Chem. Phys.* **2001**, *114*, 9244.
- (27) Storer, J. W.; Giesen, D. J.; Cramer, C. J.; Truhlar, D. G. *J. Comput.-Aided Mol. Des.* **1995**, *9*, 872.
- (28) Li, J.; Zhu, T.; Cramer, C. J.; Truhlar, D. G. *J. Phys. Chem. A* **1998**, *102*, 1820.
- (29) Winget, P.; Thompson, J. D.; Xidos, J. D.; Cramer, C. J.; Truhlar, D. G. *J. Phys. Chem. A* **2002**, *106*, 10707.
- (30) Thompson, J. D.; Cramer, C. J.; Truhlar, D. G. *J. Comput. Chem.* **2003**, *24*, 1291.
- (31) Udier-Blagovici, M.; Morales de Tirado, P.; Pearlman, S. A.; Jorgensen, W. L. *J. Comput. Chem.* **2004**, *25*, 1322.
- (32) Breneman, C. M.; Wiberg, K. B. *J. Comput. Chem.* **1990**, *11*, 361.
- (33) Singh, U. C.; Kollman, P. A. *J. Comput. Chem.* **1984**, *5*, 129.
- (34) Besler, B. H.; Merz, K. M.; Kollman, P. A. *J. Comput. Chem.* **1990**, *11*, 431.
- (35) Frisch, M. J.; Trucks, G. W.; Schlegel, H. B.; Scuseria, G. E.; Robb, M. A.; Cheeseman, J. R.; Montgomery, J. A., Jr.; Vreven, T.; Kudin, K. N.; Burant, J. C.; Millam, J. M.; Iyengar, S. S.; Tomasi, J.; Barone, V.; Mennucci, B.; Cossi, M.; Scalmani, G.; Rega, N.; Petersson, G. A.; Nakatsuji, H.; Hada, M.; Ehara, M.; Toyota, K.; Fukuda, R.; Hasegawa, J.; Ishida, M.; Nakajima, T.; Honda, Y.; Kitao, O.; Nakai, H.; Klene, M.; Li, X.; Knox, J. E.; Hratchian, H. P.; Cross, J. B.; Bakken, V.; Adamo, C.; Jaramillo, J.; Gomperts, R.; Stratmann, R. E.; Yazyev, O.; Austin, A. J.; Cammi, R.; Pomelli, C.; Ochterski, J. W.; Ayala, P. Y.; Morokuma, K.; Voth, G. A.; Salvador, P.; Dannenberg, J. J.; Zakrzewski, V. G.; Dapprich, S.; Daniels, A. D.; Strain, M. C.; Farkas, O.; Malick, D. K.; Rabuck, A. D.; Raghavachari, K.; Foresman, J. B.; Ortiz, J. V.; Cui, Q.; Baboul, A. G.; Clifford, S.; Cioslowski, J.; Stefanov, B. B.; Liu, G.; Liashenko, A.; Piskorz, P.; Komaromi, I.; Martin, R. L.; Fox, D. J.; Keith, T.; Al-Laham, M. A.; Peng, C. Y.; Nanayakkara, A.; Challacombe, M.; Gill, P. M. W.; Johnson, B.; Chen, W.; Wong, M. W.; Gonzalez, C.; Pople, J. A. *Gaussian 03 Online Manual*. [http://www.gaussian.com/g\\_ur/g03mantop.htm](http://www.gaussian.com/g_ur/g03mantop.htm) (accessed Feb 13, 2009).
- (36) Foster, J. P.; Weinhold, F. *J. Am. Chem. Soc.* **1980**, *102*, 7211.
- (37) Kelly, C. P.; Cramer, C. J.; Truhlar, D. G. *Theor. Chem. Acc.* **2005**, *113*, 133.
- (38) Olson, R. M.; Marenich, A. V.; Cramer, C. J.; Truhlar, D. G. *J. Chem. Theory Comput.* **2007**, *3*, 2046.
- (39) Easton, R. E.; Giesen, D. J.; Welch, A.; Cramer, C. J.; Truhlar, D. G. *Theor. Chim. Acta* **1996**, *93*, 281.
- (40) Marenich, A. V.; Olson, R. M.; Kelly, C. P.; Cramer, C. J.; Truhlar, D. G. *J. Chem. Theory Comput.* **2007**, *3*, 2011.
- (41) Marenich, A. V.; Cramer, C. J.; Truhlar, D. G. *J. Phys. Chem. B*, in press.
- (42) Zhao, Y.; Truhlar, D. G. *J. Chem. Phys.* **2006**, *125*, 194101.
- (43) Hariharan, P. C.; Pople, J. A. *Chem. Phys. Lett.* **1972**, *16*, 217.
- (44) Rassolov, V. A.; Pople, J. A.; Ratner, M. A.; Windus, T. L. *J. Chem. Phys.* **1998**, *109*, 1223.
- (45) Zhao, Y.; Truhlar, D. G. *Minnesota Gaussian Functional Module, version 3.0*; University of Minnesota, Minneapolis, MN, 2007.
- (46) Frisch, M. J.; Trucks, G. W.; Schlegel, H. B.; Scuseria, G. E.; Robb, M. A.; Cheeseman, J. R.; Montgomery, Jr., J. A.



- Vreven, T.; Kudin, K. N.; Burant, J. C.; Millam, J. M.; Iyengar, S. S.; Tomasi, J.; Barone, V.; Mennucci, B.; Cossi, M.; Scalmani, G.; Rega, N.; Petersson, G. A.; Nakatsuji, H.; Hada, M.; Ehara, M.; Toyota, K.; Fukuda, R.; Hasegawa, J.; Ishida, M.; Nakajima, T.; Honda, Y.; Kitao, O.; Nakai, H.; Klene, M.; Li, X.; Knox, J. E.; Hratchian, H. P.; Cross, J. B.; Bakken, V.; Adamo, C.; Jaramillo, J.; Gomperts, R.; Stratmann, R. E.; Yazyev, O.; Austin, A. J.; Cammi, R.; Pomelli, C.; Ochterski, J. W.; Ayala, P. Y.; Morokuma, K.; Voth, G. A.; Salvador, P.; Dannenberg, J. J.; Zakrzewski, V. G.; Dapprich, S.; Daniels, A. D.; Strain, M. C.; Farkas, O.; Malick, D. K.; Rabuck, A. D.; Raghavachari, K.; Foresman, J. B.; Ortiz, J. V.; Cui, Q.; Baboul, A. G.; Clifford, S.; Cioslowski, J.; Stefanov, B. B.; Liu, G.; Liashenko, A.; Piskorz, P.; Komaromi, I.; Martin, R. L.; Fox, D. J.; Keith, T.; Al-Laham, M. A.; Peng, C. Y.; Nanayakkara, A.; Challacombe, M.; Gill, P. M. W.; Johnson, B.; Chen, W.; Wong, M. W.; Gonzalez, C.; Pople, J. A. Gaussian 03, revision D.01; Gaussian, Inc., Wallingford, CT, 2004.
- (47) Olson, R. M.; Marenich, A. V.; Chamberlin, A. C.; Kelly, C. P.; Thompson, J. D.; Xidos, J. D.; Li, J.; Hawkins, G. D.; Winget, P. D.; Zhu, T.; Rinaldi, D.; Liotard, D. A.; Cramer, C. J.; Truhlar, D. G.; Frisch, M. J. Minnesota Gaussian Solvation Module, version 2008; University of Minnesota, Minneapolis, MN, 2008.
- (48) Marenich, A. V.; Hawkins, G. D.; Liotard, D. A.; Cramer, C. J.; Truhlar, D. G. GESOL, version 2008; University of Minnesota, Minneapolis, MN, 2008.
- (49) Hawkins, G. D.; Giesen, D. J.; Lynch, G. C.; Chambers, C. C.; Rossi, I.; Storer, J. W.; Li, J.; Zhu, T.; Thompson, J. D.; Winget, P.; Lynch, B. J.; Rinaldi, D.; Liotard, D. A.; Cramer, C. J.; Truhlar, D. G. AMSOL, version 7.1; University of Minnesota, Minneapolis, MN, 2004.
- (50) Dahlke, E. E.; Truhlar, D. G. MBPAC, version 2007-2; University of Minnesota, Minneapolis, MN, 2007.
- (51) Larson, L. J.; Largent, A.; Tao, F. *J. Phys. Chem. A* **1999**, *103*, 6786.
- (52) Anderson, K. E.; Siepmann, J. I.; McMurry, P. H.; Vandevondele, J. *J. Am. Chem. Soc.* **2008**, *130*, 14144.
- (53) Boys, S. F.; Bernardi, D. *Mol. Phys.* **1970**, *19*, 553.
- (54) Valiron, P.; Mayer, I. *Chem. Phys. Lett.* **1997**, *275*, 46.
- (55) Dyke, T. R.; Muentert, J. S. *J. Chem. Phys.* **1973**, *59*, 3125.
- (56) Clough, S. A.; Beers, Y.; Klein, G. P.; Rotham, L. S. *J. Chem. Phys.* **1973**, *59*, 2254.
- (57) Shostak, S. L.; Ebenstein, W. L.; Muentert, J. S. *J. Chem. Phys.* **1991**, *94*, 5875.
- (58) Sedo, G.; Schultz, J.; Leopold, K. R. *J. Mol. Spectrosc.* **2007**, *251*, 4.
- (59) Iwahori, J.; Ueda, Y.; Nakagawa, K. *J. Mol. Spectrosc.* **1986**, *117*, 1.

CT900095D